Spectrochimica Acta Part A: Molecular and Biomolecular Spectroscopy 233 (2020) 118206

Contents lists available at ScienceDirect

Spectrochimica Acta Part A: Molecular and Biomolecular Spectroscopy

journal homepage: www.elsevier.com/locate/saa

Mid-infrared spectra of dipropargyl ether ices revisited

Reggie L. Hudson [a,*], Robert F. Ferrante [b]

[a] Astrochemistry Laboratory, NASA Goddard Space Flight Center, Greenbelt, MD 20771, USA
[b] Chemistry Department, U.S. Naval Academy, Annapolis, MD 21402, USA

ARTICLE INFO

Article history:
Received 26 December 2019
Received in revised form 16 February 2020
Accepted 26 February 2020
Available online 27 February 2020

Keywords:
IR spectroscopy
IR intensities
Amorphous solids
Crystalline solids
Ices
Astrochemistry

ABSTRACT

The infrared (IR) spectrum of dipropargyl ether, $(HC{\equiv}C\text{-}CH_2)_2O$, has been reinvestigated for the compound's liquid, amorphous, and crystalline forms. The IR baseline changes and bandshape distortions seen in literature spectra have been considerably reduced by a different choice of conditions for preparing the crystalline solid, leading to the discovery of two crystalline phases of the ether. A spectrum of the liquid phase has been recorded and compared to that of the amorphous ether to check for possible procedural artifacts. To facilitate cross-laboratory comparisons, estimates are made for absorption coefficients of three IR peaks of the amorphous solid's spectrum. An interpretation is discussed for changes reported in spectral baselines and bandshapes on warming amorphous dipropargyl ether, and tests and predictions are described. The suggestion that the results from dipropargyl ether warming experiments might pose problems in applying Beer's Law to astronomical observations is addressed.

Published by Elsevier B.V.

1. Introduction

Astronomical observations of solid-phase species have included both organic (e.g., CH_3OH, CH_4) and inorganic (e.g., H_2O, CO) molecules as well as the OCN^- ion, with all identifications being made using laboratory infrared (IR) spectra. More-complex molecules and ions suspected or known to be present in cold astronomical environments are of relatively low abundance, so that an understanding of such species relies heavily on accurate laboratory spectroscopic characterization. Among recent papers concerning such work is that of Rahul and eleven co-authors on dipropargyl ether $(HC \equiv C\text{-}CH_2)_2O$ [1]. Infrared spectra of the solid amorphous ether were presented, including a description of substantial spectral changes as the amorphous ice was warmed and crystallized. The authors described these changes as "extremely unexpected" and suggested that they might complicate interpretations of astronomical observations, such as with the James Webb Space Telescope (JWST), specifically for ices of the interstellar medium.

In studying the results of Rahul et al. we have encountered multiple concerns that have motivated us to reinvestigate dipropargyl ether. First, no thickness was provided for the authors' amorphous dipropargyl ether ice that gave the IR spectrum shown. Interstellar ices are on the order of 0.1 μm in thickness, so if the authors' laboratory samples are significantly larger then the spectral changes observed on warming might be irrelevant for interstellar solids. Second, the spectrum published for amorphous dipropargyl ether had bands near 3500 and 1600 cm^{-1} that weakened substantially on warming, a change not matched by other features, raising the possibility of an experimental artifact or contamination. This was not addressed, such as by showing an IR spectrum of the ether before deposition. Third, two different spectra were provided and labeled 170 K for the crystalline ether and a table was included with thirty-seven peak positions. However, one of the IR spectra shown was little more than a sloping line and the other suffered from severely distorted bandshapes, making all peak positions uncertain. No spectra of crystalline dipropargyl ether with conventional bandshapes were provided, and we have not found a publication with such spectra.

For these reasons, it seemed desirable to reinvestigate dipropargyl ether. As we have been unable to locate a transmission IR spectrum of the liquid ether in the refereed literature, we begin by presenting one. We then show a spectrum of the amorphous solid ether for which we have estimated the thickness of the ice sample using interferometry. Next, spectra of crystalline dipropargyl ether are presented, the ices being grown using conditions chosen to minimize baseline changes and bandshape distortion. Finally, we compare our results to those in the literature and comment on possible astrochemical complications. We emphasize that our goal is not a complete vibrational analysis of dipropargyl ether, but rather the presentation of reliable, conventional IR spectra of the ether's solid forms from which such an analysis can begin and from which temperature dependent spectral changes can be investigated.

---

[*] Corresponding author.
E-mail address: reggie.hudson@nasa.gov (R.L. Hudson).

https://doi.org/10.1016/j.saa.2020.118206
1386-1425/Published by Elsevier B.V.

2. Experimental

Experiments were carried out with the same procedures and methods of our recent papers, so only a summary is needed here [2–4]. The dipropargyl ether (98% stated purity, Sigma Aldrich) received was clear, but had a distinct yellow color that was removed by bulb-to-bulb vacuum-line distillation, but which returned on standing for several days at room temperature. The ether was degassed with liquid nitrogen and multiple freeze-pump-thaw cycles. Ices were made by vapor-phase deposition onto a precooled KBr substrate in a vacuum chamber ($P_{min} \sim 10^{-7}$ Torr) at a rate that gave an increase in ice thickness of a few micrometers per hour.

Spectra were recorded from about 4000 to 500 cm^{-1} in a standard transmission mode with the IR beam perpendicular to the plane of the sample. A resolution of 2-cm^{-1} resolution was used, with little difference seen at higher resolutions.

The refractive index (n) of dipropargyl ether was given by the supplier as 1.442 ($\lambda = 590$ nm) at 20 °C and was used to estimate ice thickness and deposition rate, these quantities being determined by recording interference fringes from a laser as the ice formed [5,6]. The thickness (h) of an ice made by vapor-phase deposition is given by Eq. (1) where N_{fr} is the number of fringes recorded during deposition, $\lambda = 670$ nm for the laser, n is the ice's refractive index at 670 nm (assumed to be the same as at 590 nm), and $\theta = 3.57 \pm 0.04°$, the angle between the incident laser beam and a line drawn perpendicular to the KBr substrate. For our experimental conditions, four fringes correspond to an ice thickness of about 1 μm.

$$h = \frac{N_{fr}\lambda}{2\sqrt{n^2 - \sin^2\theta}} \approx \frac{N_{fr}\lambda}{2\,n} \tag{1}$$

We have found little information on the physical properties of dipropargyl ether, so we note here that the compound's vapor pressure was about 15 Torr at 24 °C.

CAUTION: Dipropargyl ether has a somewhat offensive smell that tends to linger in laboratories and vacuum systems after experiments are finished.

3. Results

Figs. 1–3 each show four infrared spectra of dipropargyl ether. Spectrum (a) in each case is of the reagent as received from our supplier, recorded at room temperature as a few drops between NaCl plates. Spectrum (b) is of the amorphous solid at 16 K, made at that temperature by vapor-phase deposition. From interference fringes recorded as the sample grew, we estimated the amorphous ice's thickness to be about 5.0 μm. The lower two spectra in each of our figures are for two crystalline phases of dipropargyl ether, one made by deposition at 100 K and then warming to 160 K and the other (lowest trace) by depositing at 160 K. Table 1 lists positions of some of the more-prominent peaks and shoulders.

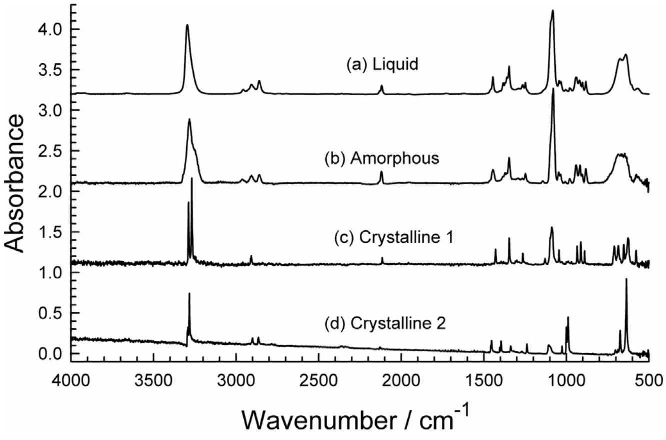

Fig. 1. Infrared spectra of dipropargyl ether as (a) a liquid at 24 °C, (b) an amorphous solid at 16 K, (c) a crystalline ice made by deposition at 100 K and then warmed to 160 K, and (d) a crystalline ice made by deposition at 160 K.

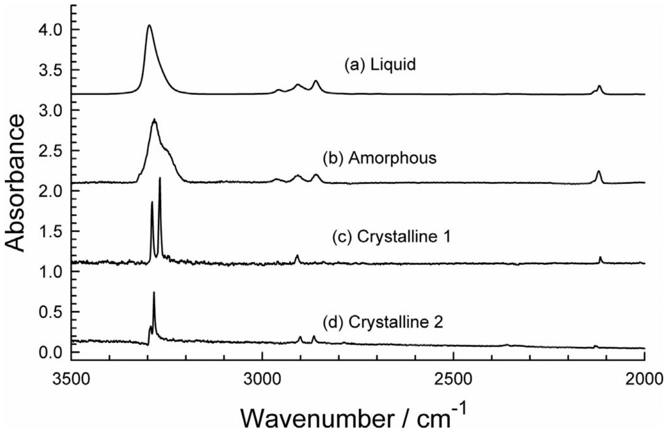

Fig. 2. Expansion of Fig. 1. Infrared spectra of dipropargyl ether as (a) a liquid at 24 °C, (b) an amorphous solid at 16 K, (c) a crystalline ice made by deposition at 100 K and then warmed to 160 K, and (d) a crystalline ice made by deposition at 160 K.

A few warming experiments were carried out in which we made an amorphous ice at 16 K and then raised its temperature to 160 K over several hours. As in the work of Rahul et al. we found that warming to about 100 K indeed changed the flat baseline's slope, raising absorbance values (lowering percent transmission) at the higher wavenumbers, but giving little change at the lower ones. However, we also found that the baseline's slope decreased by as much as 50% as the temperature approached 150 K, although the baseline never became flat (horizontal) again. Depositions at higher temperatures, such as 50, 100, and 150 K, always gave amorphous dipropargyl ether and always with flat baselines, with slopes that changed only on warming. In fact, there were few differences in amorphous-ice spectra from depositions at 16 to 150 K. Cooling amorphous ice samples never reversed the effects of warming, giving only slight sharpenings and shifts of IR bands.

Crystalline dipropargyl ether was prepared in two different ways, by warming an amorphous ice and by deposition at a temperature high enough to give a crystalline solid directly with no additional temperature change. Spectrum (c) in each of our figures shows the result of depositing dipropargyl ether at 100 K and then slowly warming to 160 K over about 2 h. From the sharpness of the peaks we assign this spectrum

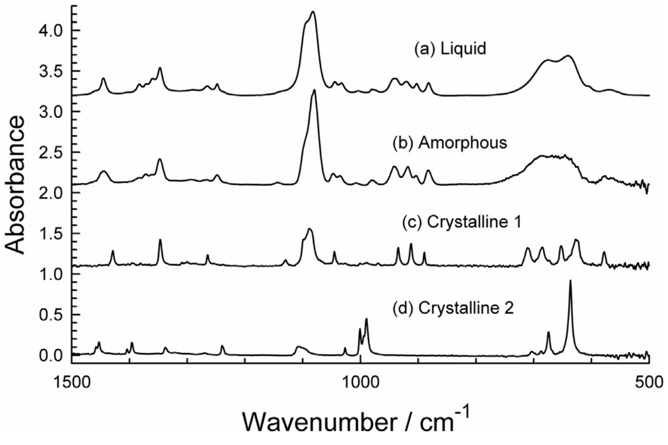

Fig. 3. Expansion of Fig. 1 showing the fingerprint region. Infrared spectra of dipropargyl ether as (a) a liquid at 24 °C, (b) an amorphous solid at 16 K, (c) a crystalline ice made by deposition at 100 K and then warmed to 160 K, and (d) a crystalline ice made by deposition at 160 K.

Table 1
Positions of selected IR features of dipropargyl ether[a].

Liquid, 24 °C (297 K)	Amorphous ice, 16 K	Crystalline ice 1, 160 K	Crystalline ice 2, 160 K
3295	3281, 3252 (sh)	3283, 3268	3295 (sh), 3292, 3284
2957, 2907, 2860	2963, 2908, 2860	2908	2901, 2865
2130 (sh), 2118	2134 (sh), 2120	2116	2130, 2126
1445	1445	1429	1458, 1453, 1404, 1396
1382, 1371, 1360, 1346	1382, 1371, 1361, 1347	1347	1338
1265, 1248	1266, 1248	1264	1239
1094 (sh), 1082	1096 (sh), 1082	1098, 1088, 1045	1107, 1097 (sh), 1027
1004, 980	1007, 981	1001, 990, 969	1001, 994, 990
941	941		
921, 903, 882	908, 903, 883	935, 913, 889	
		710	703
676, 640	685, 646	685, 653, 626, 578	687, 674, 636

[a] Positions are in units of cm^{-1}; sh = shoulder.

to crystalline dipropargyl ether. A similar result was obtained on depositing the ether at 145 K and warming to 160 K. We note here that crystallizations of amorphous ices always occurred at 154–160 K, with the lower temperature favored by slow warming. Raising the temperature of any of our ices to 164 K caused sublimation, with the time for complete removal depending on the ice's thickness.

We attempted to prepare crystalline dipropargyl ether by deposition at 170 K as in the work of Rahul et al., but the compound's vapor pressure at that temperature was too high for ice formation in our system. On lowering the substrate's temperature to 160 K and depositing for about 1 h, we obtained spectrum (d) of Figs. 1–3, which we assign to a second crystalline phase. In a few depositions at lower temperatures, such as 150 K, warming the resulting ices gave IR spectra that were a mixture of the two crystalline forms of Figs. 1–3. It was impossible to determine crystalline ice thicknesses in our work as either weak or no interference fringes were seen during depositions at 160 K and above, suggesting that the refractive index of the ice at that temperature was close to that of our substrate (n_{KBr} ~ 1.5).

In a different type of experiment, we prepared the crystalline ice of Fig. 1(c) and held it at ~155 K for several hours. Inevitably, the spectrum began to change to that of Fig. 1(d), and the change proved to be irreversible. Unfortunately, sublimation complicated efforts to quantify the crystalline-crystalline transition. All attempts at converting the spectrum of Fig. 1(d) into that of Fig. 1(c) failed, such as by varying deposition rate, ice thickness, and warming rate.

As a final experiment, we co-deposited H_2O and dipropargyl ether at 16 K, using separate deposition lines, to give an ice with a 10:1 H_2O: ether molecular ratio. The sample's IR spectrum was scarcely different from that of amorphous H_2O-ice, with only a few ether peaks even barely visible. Warming this amorphous mixture gave no significant changes in the spectrum's baseline, and none were expected based on previous work with H_2O-ice [7,8].

4. Discussion

4.1. Infrared spectra - liquid and amorphous dipropargyl ether

The similarity of our spectra for liquid (24 °C) and amorphous (16 K) dipropargyl ether in Figs. 1–3 is obvious, suggesting that no new IR peaks were introduced by vapor-phase condensation. The bands of Rahul et al. near 3500 and 1600 cm^{-1} [1] are not present in our spectra, the latter peak suggestive of a C═C vibration, perhaps from a partial polymerization of the starting material that reduced one of the compound's triple bonds to a double bond. Infrared bands near 3500 and 1600 cm^{-1} could also be due to contamination by H_2O-ice, which would explain why they disappeared from the spectra at a lower temperature than the much heavier dipropargyl ether molecules. Except for those two IR features, our spectrum of amorphous dipropargyl ether resembled that of Rahul et al., as did some of the change in the baseline's slope on warming. Peak positions are similar to those tabulated by the same authors.

Assignments of each peak in our liquid-phase and amorphous-ice spectra were not attempted, but some general comments can be made. Absorption features near 3281 and 3252 cm^{-1} can be assigned to the two acetylenic ≡C-H stretching fundamentals, while peaks in the 3000–2800 cm^{-1} region belong to CH_2 stretches, again fundamentals. Molecules such as butadiyne (diacetylene, HC≡C-C≡CH) and cyanogen (N≡C-C≡N) with two terminal groups of the type C≡C or C≡N can show both symmetric and asymmetric C≡X stretches. In three of the spectra in our figures, two weak features separated by about 13 cm^{-1} were seen near 2125 cm^{-1} in the C≡C stretching region, but only one C≡C peak was seen for spectrum (c). This suggests that there is little or no dipole moment change accompanying one of the two C≡C vibrations, such as the symmetric one, for the phase formed by slowly warming the amorphous ether from 100 K to give spectrum (c). Various deformations, rockings, and twistings are in the fingerprint region (~1500–500 cm^{-1}), Fig. 3, the large peak near 1100 cm^{-1} belongs to one or more C—O stretches, and a broad feature below 700 cm^{-1} can be associated with ≡C-H bendings. Substantial overlap among the many peaks of the 3 N - 6 = 33 possible fundamentals, plus the usual combinations, differences, overtones, and mixing of modes, leads to considerable difficulty in making firm assignments of many peaks, and no further attempt was made in that direction.

Some guidance in IR peak assignments might be possible from modern computational-chemistry methods, such as those of Rahul et al. [1], but the results in that paper do not include a description of the optimized geometry, such as the orientations of the molecule's propargyl groups, making it difficult to compare the calculated intensities with those we observed. Aside from structural considerations, the two intense IR features at 3300–3200 cm^{-1} that were assigned by the authors to combination bands are more likely due to fundamental vibrations, which are expected to be much stronger than combination features. Conversely, a peak listed at 3061 cm^{-1} and assigned to a fundamental vibration in the authors' Table 1 is so weak in the figures that it cannot be seen. Unfortunately, the extensive overlap of five spectra of amorphous dipropargyl ether in the authors' Figure 1 hinders a better comparison to our own results.

Given the approximate thickness of 5.0 μm for the 16-K ice of Fig. 1 (b), we estimated apparent absorption coefficients of $\alpha'(3281\ \text{cm}^{-1}) = 3530\ \text{cm}^{-1}$, $\alpha'(2120\ \text{cm}^{-1}) = 668\ \text{cm}^{-1}$, and $\alpha'(1082\ \text{cm}^{-1}) = 5350\ \text{cm}^{-1}$. These α' values allowed us to calculate that the deposition rate of Rahul et al. was about 20 times higher than that of the present work.

4.2. Infrared spectra - crystalline dipropargyl ether

The temperature at which the amorphous ices of Rahul et al. [1] crystallized is unclear. A phase transition temperature of 170 K is cited in the abstract, but the 170-K spectrum of the authors' Figure 1 is almost featureless. That paper's Figure 2 shows spectra for an ice made at 170 K, with first-derivative-like bandshapes and a severely distorted baseline, two undesirable spectral effects associated with IR scattering by a solid sample. See particularly the literature on artifacts in IR spectra of solids, such as that concerning anomalies from scattering and from non-homogeneous solid samples [9]. Scattering varies inversely with wavelength, and so the higher-wavenumber part of a baseline will be influenced the most, as observed. Such effects are well known and plague, among other areas, IR studies of circumstellar and interstellar dust [10], work with biomaterials [11], and spectra of minerals [12]. As a specific example, in the study of Chou et al., the authors' Figure 5 shows that as particle size increases, extinction rises on the high-wavenumber end of the spectrum, similar to what is seen when amorphous dipropargyl ether is warmed, and consistent with some form of aggregation or association taking place in the ether samples [13]. The cracking of an ice on warming might also introduce inhomogeneities, altering a spectral baseline and changing spectral contrast.

Unlike our results with amorphous ices, our crystalline ices had spectra that differed substantially from those of Rahul et al. The baselines of our crystalline-ice spectra showed little non-zero slope, and only a hint of a derivative bandshape, such as the absorbance at ~3300 cm^{-1} at the bottom of Fig. 2. The small dip on the high-wavenumber side and the slow decline to the baseline on the opposite side are reminiscent of anomalous dispersion in IR spectra of solids and suggest that the nature of the crystalline-ice sample is different from that of the amorphous solid, such as in particle (i.e., crystallite) size, refractive index, or both. These effects are much more pronounced in the spectra of Rahul et al., perhaps influenced by the much faster rate of ice formation or the greater heating rate (5 K min^{-1} vs. 0.5 K min^{-1}). Even slower rates for ice growth or warming might reduce the baseline changes even more.

In our recent studies of crystalline thiols and nitriles we were aided by earlier results from calorimetric, diffraction, and closed-cell IR measurements [14–16]. Unfortunately, no such published work is available for dipropargyl ether, making it difficult to extract structural details for the compound's crystalline phases from IR spectra alone. Differences certainly are seen in spectra (c) and (d) of our figures, and undoubtedly are connected to crystal structure and molecular conformation. For example, for the acetylenic C—H stretches seen near 3300 cm^{-1}, two peaks of comparable intensities are found in one spectrum, but not the other. Possible variations in the two -C≡C-O-C dihedral angles also complicate assignments and extraction of structural details. See the work of Durig et al. on methyl propargyl ether, $\text{H-C≡C-CH}_2\text{-O-CH}_3$, for results on a related molecule [17].

It is difficult to say which of the two crystalline phases we prepared at 160 K is the more stable at that temperature. However, the IR spectra labeled (c) in our figures more closely resembles spectrum (a) of the liquid than (d) does, and so we are inclined to think of (c) as for the high-temperature phase of the crystalline ether, leaving (d) to be for the low-temperature polymorph, which is the more stable form at 160 K. Additional evidence for this interpretation is that spectrum (d), once reached, never was seen to convert into spectrum (c), but the reverse certainly was observed. That the high-temperature phase is the first to form on crystallization of the amorphous solid simply indicates that it is the kinetically favored polymorph. See also the work of Tizek et al. on the Ostwald Step Rule and CH_3CN crystallization for more information [18].

4.3. Spectral changes on warming

The observed sloping baseline seen in some of our crystalline ices and in spectra of warmed amorphous dipropargyl ether suggest some type of ice cracking, sample non-uniformity, or perhaps aggregation (association) among the ice's molecules. We know of no such spectral changes on warming either acetylene (HC≡CH) or propyne (HC≡C-CH_3), but we have seen a small baseline change on warming propargyl alcohol ($\text{HC≡C-CH}_2\text{-OH}$), which is known to form dimers [19]. Therefore, greater changes for the more-complex dipropargyl ether, $\text{HC≡C-CH}_2\text{-O-CH}_2\text{-C≡CH}$, are not altogether surprising. We feel confident in predicting similar baseline changes for related solids, such as amorphous propargyl amine ($\text{HC≡C-CH}_2\text{-NH}_2$) and methyl propargyl ether ($\text{HC≡C-CH}_2\text{-O-CH}_3$).

A possible result of molecular association on warming is that as aggregates or dimeric species begin to form then their larger size could produce electronic absorbance increases at longer wavelengths at the expense of absorbance at shorter wavelengths. It might be possible to observe such changes by examining the UV–visible spectrum of dipropargyl ether on warming the amorphous solid. The vacuum-UV spectra of Rahul et al. [1] indeed shows substantial absorbance changes for one peak (~140 nm) on warming and a slight change at another (~192 nm), but with a spectral range of only about 110 nm it is impossible to determine if a new band appeared with $\lambda > 220$ nm, such as might correspond to the yellow color already mentioned. Spectra over a wider wavelength range are needed.

Finally, we note again that the initial spectra for dipropargyl ether ices always showed flat baselines and conventional bandshapes, and only on warming did large changes appear. We suspect that the molecules in ices made at the higher temperatures were closer to an equilibrium configuration and homogeneous distribution than those made at the lower temperatures, due to both the higher deposition temperature and the heat released on condensation. The possible influences of warming rates, deposition temperatures, deposition rates, and even the substrate on which the ice is grown remain to be explored.

4.4. Astrochemical complications?

Using results from amorphous dipropargyl ether work, it has been suggested that interpretations of interstellar-ice spectra could be complicated by large baseline shifts being mistaken for high molecular abundances [1]. Such complications would render the application of Beer's Law questionable, but there are at least two reasons why such concerns can be set aside. First, interstellar ices are dominated by molecules, such as H_2O, CO_2, and CH_3OH, that are far more abundant than propargyl ethers, and these more-abundant molecules are not known to produce any of the baseline shifts and distorted bandshapes seen on warming dipropargyl ether. Indeed, IR spectra of our H_2O-rich ice doped with dipropargyl ether showed no baseline changes on warming. Second, the thickness of the dipropargyl ether ices used to observe such distorted baselines [1] was on the order of 5 μm, based on comparisons with our own IR spectra. The scattering effects from any such laboratory samples will be far greater than those of interstellar ices, which are much smaller (~0.1 μm). We know of no astrochemical theory that predicts a substantial amount of dipropargyl ether or similar molecule in an interstellar ice, but in any case H_2O and other molecules would interfere with the aggregation of dipropargyl ether, preventing the sort of baseline changes and distorted bandshapes described here and in Rahul et al. [1].

On the interpretation given here and from current astrochemical theory there is no reason to expect new problems when using Beer's Law to help interpret telescopic or spacecraft data on ices from past, present, and future IR observations. In a sense, of course, there are no exceptions to Beer's Law, only applications outside its domain, such as to samples that scatter incident light, are inhomogeneous, or are composed of entities (e.g., molecules) that do not absorb independently. These complications are well known to chemists and others, such as planetary scientists studying the moons of the outer Solar System. At present there seems to be no reason for concern that new and unknown baseline shifts will reduce the value of Beer's Law.

4.5. Future work

We do not intend to continue this line of research with dipropargyl ether, but we can envision multiple areas for future work, such as the following:

- Accurate measurements of density and refractive index of dipropargyl ether
- Measurements of band strengths, absorption coefficients, and optical constants
- Crystallographic study to determine the relative orientation of the propargyl groups
- Vapor pressures of crystalline dipropargyl ether
- Enthalpy of sublimation of crystalline dipropargyl ether

- Closed-cell IR measurements to better understand the two crystalline phases and the kinetics of the conversion of one form into the other
- A detailed study of dipropargyl ether's IR features in the presence of other solids, such as H_2O
- Computational studies to determine the relative energies and barriers between the various conformational isomers of dipropargyl ether
- A more-detailed vibrational analysis with the benefit of isotopologs
- IR studies of other propargyl compounds, such as propargyl amine, to continue investigating the structural changes seen with dipropargyl ether

4.6. Summary and conclusions

Mid-IR spectra of dipropargyl ether have been presented for the compound's solid and liquid phases, the latter apparently for the first time. The earlier spectrum of the amorphous solid has been verified, as have some baseline shifts on warming the sample. Spectra of two crystalline phases have been recorded, one for the first time, and each with far less spectral distortion and greater spectral contrast than in earlier work. An interpretation of some previously published results has been described, astrochemical connections discussed, and a few predictions and ideas offered for future work involving organic molecules with one or more propargyl groups.

CRediT authorship contribution statement

Reggie L. Hudson: Conceptualization, Methodology, Writing - original draft. **Robert F. Ferrante:** Conceptualization, Methodology, Writing - original draft.

Declaration of competing interest

The authors declare that they have no known competing financial interests or personal relationships that could have appeared to influence the work reported in this paper.

Acknowledgments

Support from the NASA Astrobiology Institute through funding awarded to the Goddard Center for Astrobiology under proposal 13-13NAI7-0032 is acknowledged. Support also was received from NASA's Planetary Science Division Internal Scientist Funding Program through the Fundamental Laboratory Research (FLaRe) work package at the NASA Goddard Space Flight Center. Yuki Yarnall (NASA NPP) is thanked for assistance with liquid-phase spectra.

References

[1] K.K. Rahul, J.K. Meka, S. Pavithraa, P. Gorai, A. Das, J.-I. Lo, B.N.R. Sekhar, B.-M. Cheng, P. Janardhan, A. Bhardwaj, N.J. Mason, B. Sivaraman, Infrared attenuation due to phase change from amorphous to crystalline observed in astrochemical propargyl ether ices, Spectrochim. Acta 224 (2020), 117393.

[2] R.L. Hudson, P.A. Gerakines, M.H. Moore, Infrared spectra and optical constants of astronomical ices: II. Ethane and ethylene, Icarus 243 (2014) 148.

[3] P.A. Gerakines, R.L. Hudson, The infrared spectra and optical constants of elusive amorphous methane, Astrophys. J. 805 (2015) L20.

[4] R.L. Hudson, P.A. Gerakines, R.F. Ferrante, IR spectra and properties of solid acetone, an interstellar and cometary molecule, Spectrochim. Acta 193 (2018) 33.

[5] O.S. Heavens, Optical Properties of Thin Solid Films, 2nd edition Dover, New York, 2011 114 (Original printing: 1955, Butterworths Scientific Publ. London).

[6] P. Groner, I. Stolkin, H.H. Günthard, Measurement of deposition rate in matrix spectroscopy with a small laser, J. Phys. E Sci. Instrum. 6 (1973) 122.

[7] D.M. Hudgins, S.A. Sandford, L.J. Allamandola, A.G.G.M. Tielens, Mid- and far-infrared spectroscopy of ices: optical constants and integrated absorbances, Astrophys. J. Suppl. Ser. 86 (1993) 713.

[8] M.M. Maldoni, R.G. Smith, G. Robinson, V.L. Rookyard, A study of the 2.5 - 25 μm spectrum of H_2O ice, Mon. Not. R. Astron. Soc. 298 (1998) 251.

[9] J.M. Chalmers, Mid-infrared spectroscopy: anomalies, artifacts and common errors, in: P.R. Griffiths, J.M. Chalmers (Eds.), Handbook of Vibrational Spectroscopy, John Wiley & Sons, Ltd, Chichester, UK 2006, p. 2327.

[10] A.M. Hofmeister, E. Keppel, A.K. Speck, Absorption and reflection infrared spectra of MgO and other diatomic compounds, Mon. Not. R. Astron. Soc. 345 (2003) 16.

[11] A. Dazzi, A. Deniset-Besseaua, P. Lasch, Minimising contributions from scattering in infrared spectra by means of an integrating sphere, Analyst 138 (2013) 4191.

[12] O. Laskina, M.A. Young, P.D. Kleiber, V.H. Grassian, Infrared extinction spectra of mineral dust aerosol: single components and complex mixtures, J. Geophys. Res. 117 (2012) D18210.

[13] C.C.-K. Chou, S.-H. Huang, T.-K. Chen, C.-Y. Lin, L.-C. Wang, Size-segregated characterization of atmospheric aerosols in Taipei during Asian outflow episodes, Atmos. Res. 75 (2005) 89.

[14] R.L. Hudson, Infrared spectra and band strengths of CH_3SH, an interstellar molecule, Phys. Chem. Chem. Phys. 18 (2016), 25756.

[15] R.L. Hudson, P.A. Gerakines, Infrared spectra and interstellar sulfur: new laboratory results for H_2S and four malodorous thiol ices, Astrophys. J. 867 (2018) 1.

[16] R.L. Hudson, Preparation, identification, and low-temperature infrared spectra of two elusive crystalline nitrile ices, Icarus 338 (2020), 113548.

[17] J.R. Durig, Q. Tang, H.V. Phan, Conformational stability, ab initio calculations and methyl propargyl ether, J. Mol. Struct. 320 (1994) 193.

[18] H. Tizek, H. Grothe, E. Knözinger, Gas-phase deposition of acetonitrile: an attempt to understand Ostwald's step rule on a molecular basis, Chem. Phys. Lett. 383 (2004) 129.

[19] J. Saini, K.S. Viswanathan, Discerning near-isoergic isomers. A matrix isolation infrared and *ab Initio* study of the propargyl alcohol dimers, J. Phys. Chem. A 121 (2017) 1448.